Saturation of front propagation in a reaction diffusion process describing plasma damage in porous low-k materials

Safaverdi, S.; Barkema, G.T.; Kunnen, E.; Urbanowicz, A.M.; Maes, C.

Note: To cite this publication please use the final published version (if applicable).

Saturation of front propagation in a reaction diffusion process describing plasma damage in porous low-*k* materials

Soghra Safaverdi,[1] Gerard T. Barkema,[2,3] Eddy Kunnen,[4] Adam M. Urbanowicz,[5] and Christian Maes[1]

[1]*Instituut voor Theoretische Fysica, K.U. Leuven, Belgium*
[2]*Theoretical Physics, Utrecht, The Netherlands*
[3]*Instituut-Lorentz for Theoretical Physics, Leiden University, The Netherlands*
[4]*imec, Kapeldreef 75, B-3001 Heverlee, Belgium*
[5]*Semiconductor Physics Section, Department of Physics and Astronomy, K.U. Leuven, Belgium*

We propose a three-component reaction-diffusion system yielding an asymptotic logarithmic time dependence for a moving interface. This is naturally related to a Stefan problem for which both one-sided Dirichlet-type and von Neumann-type boundary conditions are considered. We integrate the dependence of the interface motion on diffusion and reaction parameters and we observe a change from transport behavior and interface motion $\sim t^{1/2}$ to logarithmic behavior $\sim \ln t$ as a function of time. We apply our theoretical findings to the propagation of carbon depletion in porous dielectrics exposed to a low temperature plasma. This diffusion saturation is reached after about one minute in typical experimental situations of plasma damage in microelectronic fabrication. We predict the general dependencies on porosity and reaction rates.

I. INTRODUCTION

The generation and propagation of interfaces in reaction-diffusion systems is of great importance in a variety of scientific and technological contexts. In nature, the interface often spatially separates two macroscopically different homogeneous regimes in which one phase or product dominates another one. Typically, at least one particle type diffuses through the medium while reacting with other particles. Births and deaths depend on the spatial location and on the presence of other particle types. Then, when installing appropriate initial and boundary conditions one often sees the appearance of an interface and one asks for the typical temporal behavior in its initial growth and further propagation. The case we treat here is boundary driven from one side, with symmetric bulk diffusion for one particle type that invades the region of a second particle type, while constantly being annihilated by yet a third type of particle. That creates a moving phase boundary and thus goes under the general name of the Stefan problem.[1,2]

The present work is inspired by experimental investigations on plasma damage in porous low-capacitive materials (low-*k*, see Ref. 3). One imagines here a porous SiOC material which is exposed via one of its physisorbedaries to radicals such as active oxygen atoms. These radicals diffuse through the material while removing hydrophobic carbon-hydrogen groups and while being chemi-adsorbed in the pores of the material. One then observes the appearance and motion of an interface separating a rich (pristine) carbon-phase from a damaged (oxygen-rich) layer. It is important here to understand the time dependence of that motion and its dependence on diffusion and reaction parameters, which can further be related to material and chemical properties. We come back to this application in the separate Sec. IV.

Of course, the literature on interface motion from reaction-diffusion equations is vast, and many different phenomena have been reported. In particular, damage spreading and related front propagation can take many different forms which we cannot at all review here (see, e.g., Refs. 4–6 for general research aspects). As just one very famous example for one-dimensional front propagation, as we also have here, reaction-diffusion equations such as of the type of Kolmogorov-Petrovsky-Piskounov show interface motion between two homogeneous phases at constant speed.[7] That then takes the form of traveling waves in which one phase advances over the other phase. Here, however, the proposed model shows the motion of the interface $x(t) \simeq \ln(1 + at + b\sqrt{t})$ (in one dimension as a function of time t) to be logarithmic, which means that after an initial period diffusion saturation occurs. The main point is that the diffusive motion is boundary driven and that the propagation is limited by the reactions. For the purpose of the application, the logarithmic behavior is caused by the disappearance of the oxygen radicals before reaching the moving interface separating them for the carbon-rich environment. The $\sqrt{t}$ within the logarithm, mostly visible in an initial time period, originates directly from the diffusive motion.

The next section contains the specific mathematical model in the form of coupled partial differential equations. They give a mean-field description of the reaction-diffusion system. The main finding is the change from a diffusive to a specific logarithmic time dependence for the interface $x(t)$ as above, with the study of dependencies on initial conditions and dynamical parameters. We give a physical heuristics for understanding the basic characteristics via a linearized model.
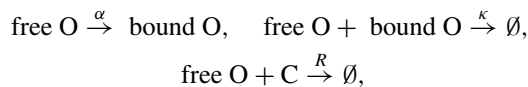
Section III on numerical results summarizes the behavior of our model as a function of the physical parameters. Our results agree with the analytical results of the linearized model, but the higher flexibility of simulations allow for obtaining additional information and predictions concerning the dependence on the various parameters in the model.

Section IV goes deeper into the specific application that triggered our study, that of the propagation of damage in porous low-*k* materials. We recall the main aspects and the meaning of our result for that context. In particular, Ref. 8

contains already the basic set of differential equations, but no systematic analysis was performed and the distinction between different (one-sided) boundary conditions was not considered. The present paper also adds the interesting connections with reaction-diffusion systems of the Stefan type.

II. MODEL AND MAIN FINDINGS

There are three types of particles. The first are called free O particles, which can diffuse but can also change into bound O particles and further annihilate with either bound O particles or with C particles

$$\text{free O} \xrightarrow{\alpha} \text{bound O}, \quad \text{free O} + \text{bound O} \xrightarrow{\kappa} \emptyset,$$
$$\text{free O} + \text{C} \xrightarrow{R} \emptyset,$$

and no other reactions or diffusions take place. The letters are chosen in the context of the later application in Sec. IV with O for oxygen and C for carbon. The word "free" will there be understood as "reactive" and "bound" will mean adsorbed to the inner surface, either physically or chemically. Once oxygen atoms are absorbed on the surface they start to move around until they recombine and desorb. In other words, since in the experimental conditions desorption of bounded oxygen molecules typically occurs through recombination, reversible desorption is not taken into account.[9,10] For the moment we continue to use the more general words "free" and "bound," as the mathematical setup can have different natural realizations.

The dynamics is further determined by the initial condition at time zero when there are only C particles with homogeneous density and by the boundary conditions. The physics we have in mind concerns a three-dimensional region of locations ($x \geqslant 0, y, z$), which is isotropic over the (y, z) coordinates. For the boundary conditions at the $x = 0$ plane we consider two possibilities. The first, of Dirichlet type, specifies a constant density of free O particles at $x = 0$; the second, of von Neumann type, gives a constant flux of particles entering the region at $x = 0$. For the questions and the problem at hand we restrict ourselves to an effective mean-field treatment, ignoring fluctuations or microscopic inhomogeneities, and the geometry is one-dimensional.

We consider the coordinate $x \geqslant 0$ in which to express the profile of particle densities as a function of time $t \geqslant 0$. There are thus three types of concentrations $\rho(x,t)$, $c(x,t)$, and $m(x,t)$, respectively, for free O particles, C particles, and bound O particles. The reaction-diffusion system is then defined via the equations

$$\dot{\rho} = D\rho'' - \kappa\rho m - Rc\rho - \alpha\rho,$$
$$\dot{c} = -Rc\rho, \quad (1)$$
$$\dot{m} = -\kappa\rho m + \alpha\rho,$$

where the dotted left-hand sides are time derivatives. The concentration ρ (of the free O particles) undergoes a second spatial derivative in the right-hand side of the first line of Eq. (1); the parameter $D > 0$ being the diffusion constant. The other parameters κ, R, and α are positive reaction rates.

The initial condition ($t = 0$) specifies

$$c(x,t=0) = 1, \quad \rho(x,t=0) = m(x,t=0) \equiv 0, \quad \text{for} \quad x > 0,$$
$$(2)$$

meaning that we start with C particles fully occupying the material. On the other hand, the boundary conditions ($x = 0$) can be taken either

Dirichlet type: $\rho(x = 0, t) = V,$

or von Neumann type: $\rho'(x = 0, t) = -J,$ (3)

where we can take $V = 1$ without loss of generality; the $J > 0$ stands for the rate of free O particles entering the region, which for the moment we leave as a parameter. It seems more natural to opt for von-Neumann-type boundary conditions for the specific application we have in mind, but we checked that after a transient time there is really no difference between Dirichlet and von Neumann conditions. In the case of von-Neumann-type boundary conditions, the value $\rho(x = 0, t)$ converges from being zero at time zero to a fixed finite value (equal to some $V > 0$ depending on J) exponentially fast as time evolves. As a consequence, we mostly concentrate on just one type, that of Dirichlet boundary conditions with $\rho(x = 0, t) = 1$ for all times, but further discussion on possible differences will follow below.

The results of numerical integration of the differential equations (1) are detailed in Sec. III. Our main finding is that the concentration $c(x,t)$ of C-particles (defining the absence of damage in the application of Sec. IV) shows an interface $x(t)$ separating a C-poor from a C-rich phase. There are *a priori* a number of different possible mathematical definitions of the position of the interface $x(t)$. A first one is to solve $c(x(t),t) \simeq 1/2$ (or some other number) for $x(t)$, which certainly makes sense when the interface is sharp enough, after some transient time, but is less useful for very small times. A second definition uses the same conditions as above, but we add the equation $\dot{x}(t) = -D\rho'[x(t),t]$ for the interface speed. That brings the problem in the natural neighborhood of Stefan problems,[1,2] also valid for very small times but more involved numerically. Whatever (reasonable) definition we take for $x(t)$ we invariably find that the motion is logarithmic of the general form $x(t) = A\ln(1 + at + b\sqrt{t})$ in a typical range of parameters for diffusion and reaction rates D, κ, R, and α. The coefficients A, a, and b depend on these parameters, see also in Sec. III. For small times the motion is diffusive $x(t) \sim \sqrt{t}$ while it saturates as $x(t) \sim \ln t$ for large times t. The transition between the two regimes is basically determined by the amount of reactivity, the more the O particles can be annihilated, the faster saturation sets in.

An approximate treatment toward the second Stefan-like definition of the interface motion described above can already be made visible for a much simpler linear system to which we turn next. We simplify Eq. (1) to a one-component reaction-diffusion equation by imagining an autonomous linear dynamics for ρ of the form

$$\dot{\rho}(x,t) = D\rho'' - \beta\rho. \quad (4)$$

Equation (4) mimics the first line of Eq. (1) in the approximation $\kappa m + Rc + \alpha = \beta > 0$ constant, which we expect to be mostly reasonable when $c = 0$ and $m = \text{constant}$, which

makes sense in the damaged region $[0 < x < x(t)]$ where the carbon was depleted. The right boundary denoted by ℓ in what follows therefore plays the role of interface. We also can think of β as a measure of reactivity and interaction, while D measures the diffusion. The main advantage is, of course, that now Eq. (4) can be solved exactly with boundary conditions $\rho(x=0,t)=1, \rho(x=\ell,t)=0$ and initially $\rho(x,t=0)=0$. The solution is

$$\rho(x,t) = \rho_\ell(x) + e^{-\beta t}\sum_1^\infty a_n \, e^{-\frac{Dn^2\pi^2}{\ell^2}t}\,\sin\frac{n\pi}{\ell}x, \quad \text{where}$$

$$\rho_\ell(x) = \frac{1}{1-e^{2k\ell}}e^{kx} + \frac{1}{1-e^{-2k\ell}}e^{-kx}, \quad k \equiv \sqrt{\beta/D}$$

$$= -\sum_1^\infty a_n \sin\frac{n\pi}{\ell}x \quad \text{which determines the } a_n, \quad (5)$$

and ρ_ℓ is the stationary solution on $[0,\ell]$. In fact we see that $\rho(x,t)$ converges exponentially fast to ρ_ℓ with rate $\beta > 0$ uniformly in ℓ. We can already learn a great deal from the behavior at the edge $x = \ell$. It is easy to find that

$$\rho'_\ell(\ell) = \frac{-k}{\sinh k\ell}. \quad (6)$$

We think now of ℓ as the position x of the interface and $-\rho'_\ell(\ell)$ is then the speed of the interface, so that Stefan's condition $\dot{x}(t) = D\,k/\sinh[kx(t)]$ can be integrated to give

$$x(t) = \sqrt{\frac{D}{\beta}}\,\ln[1 + \beta t + \sqrt{2\beta t + \beta^2 t^2}]. \quad (7)$$

We clearly recognize the behavior $x(t) \propto \sqrt{D/\beta}\,\ln t$ for large times t resulting in a straight line in Fig. 1 and intersecting the vertical axis (small t) at $\sqrt{D/\beta}\,\ln(2\beta)$. For small times t Eq. (7) gives $x(t) \propto \sqrt{t}$ and $x(t=1) \simeq \sqrt{2D}$ for small $\beta > 0$. We can thus find the effective D and β for Eq. (4) from the intersections of the $x(t)$ as a function of $\ln t$ with the vertical axis, as in Fig. 1, which provide consistency checks for our modeling equations.
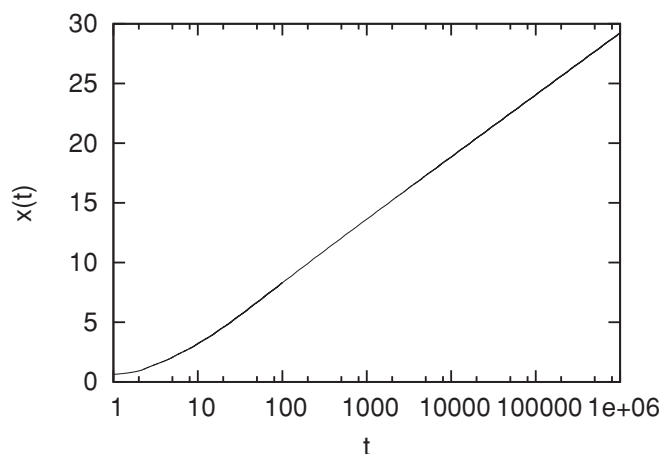

FIG. 1. Position of the interface $x(t)$ as a function of time. For longer times, the curve approaches a straight line, indicating that asymptotically $x(t) = A\ln(1 + at)$.

Similarly, we can also solve Eq. (4) with von-Neumann-type boundary condition $\rho'(x=0,t)=-J$ but still putting $\rho(x=\ell,t)=0$ and initially $\rho(x,t=0)=0$. The solution is

$$\rho(x,t) = \rho_s(x) + e^{-\beta t}\sum_1^\infty b_n \, e^{-\frac{D(n-1/2)^2\pi^2}{\ell^2}t}\,\cos\frac{(n-1/2)\pi}{\ell}x,$$

where

$$\rho_s(x) = \frac{J}{k}\left[\frac{e^{-kx}}{1+e^{-2k\ell}} - \frac{e^{kx}}{1+e^{2k\ell}}\right], \quad (8)$$

$$k \equiv \sqrt{\beta/D} = -\sum_1^\infty b_n \cos\frac{(n-1/2)\pi}{\ell}x$$

which determines the b_n.

Exponentially fast in time t, $\rho(0,t) = J/k + O(e^{-k\ell})$, and hence we find that for $J \sim \sqrt{\frac{\beta}{D}}$ the von Neumann condition imitates the Dirichlet condition with fixed $\rho(0,t)=1$ and $\rho_\ell(x) \simeq \rho_s(x) \simeq \exp{-kx}$ for large ℓ, at least for $\beta \neq 0$. Clearly then, when the rate β would go to zero, some differences between Dirichlet and von Neumann (one-sided) boundary conditions can be expected, as we indeed recover in Sec. III B for the real model. The next section goes back to the full nonlinear model equations (1), but we will find the many general features to be similar to our chosen approximation above.

III. NUMERICAL RESULTS

We now turn to the full set of Eq. (1), and switch to computer simulations. First, we study the system for a specific set of parameters $D = 1.0$, $\kappa = 0.1$, $R = 1.0$, and $\alpha = 0.1$, and apply Dirichlet boundary conditions; the primary motivation for this specific choice of the parameters lies in their numerical convenience. We apply a forward Euler integration scheme to Eq. (1) with a time step of $\Delta t = 0.001$, and store the density profiles of C particles, free and bound O particles at times $t = 1,2,\ldots$. Based on our analytic solution (7) of the simplified description (4), we expect that for long times the interface position $x(t)$, defined as the (linearly interpolated) location where the C-particle density equals 1/2, changes in time as $x(t) \approx A\ln(1 + at)$, for some values of A and a which are determined by the system parameters D, κ, R, and α. Figure 1 shows that this expected long time behavior is confirmed by the simulation data.

In the same simulations, we also determined the concentrations of C particles and free O particles as a function of position, for the times $t/100 = 1,2,4,8,\ldots,8192$. These are $c(x,t)$, respectively, $\rho(x,t)$ in Eq. (1). The resulting profiles of C concentration are shown in Fig. 2(a). The C-density profile attains a sigmoid-like shape, which gradually moves deeper into the material. As the times of the curves are separated by a factor of 2, and the depth increases with the logarithm of time, the curves are more or less equidistant.

The concentration profile of free O particles is shown in Fig. 2(b). The general shape is that of an exponentially decaying curve up to the interface position $x(t)$, after which it decays again exponentially, but with a much steeper slope. Once the interface has significantly moved into the material, the gradient of free O concentration at the surface
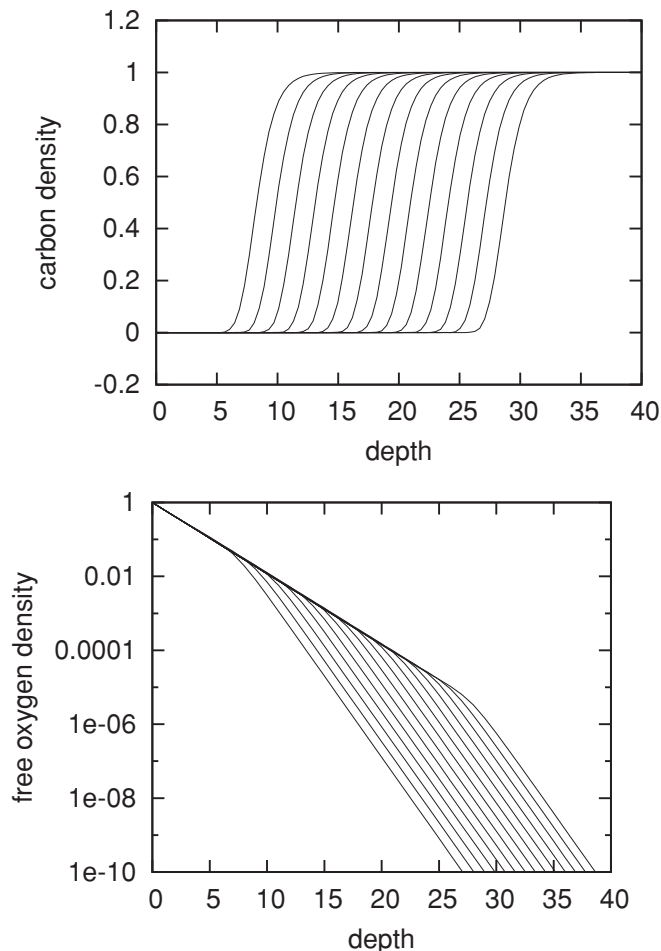
FIG. 2. Profile of the C concentration (top panel) and free O concentration (lower panel) as a function of depth, at times $t/100 = 1, 2, 4, \ldots, 8192$. Note that the top panel has a linear vertical scale, while the lower panel has a logarithmic vertical scale.

becomes constant even though we applied Dirichlet boundary conditions. This confirms our earlier analytic observation that the behavior for Dirichlet and von Neumann conditions soon becomes indistinguishable.

A. Influence of diffusion

An important ingredient is to understand the influence of the diffusion constant D on the temporal behavior of the interface. After all, the porosity and the architecture of the material can modify exactly that diffusive behavior.

We repeated the simulations with different values for the diffusion coefficient: $D = 0.5, 1, 2$, and 4. Figure 3 shows the rescaled interface position $x(t)/\sqrt{D}$, indicating that the main effect of variations in D is a rescaled amplitude: $A \sim \sqrt{D}$, as expected from the linear model in Eq. (7). It appears therefore that we understand the influence of the connectivity of the porous material on the time dependence of the interface.

B. Influence of reactivities

The adsorption of the free O-particles and the chemical annihilation of the free O-particles with the bound O-particles
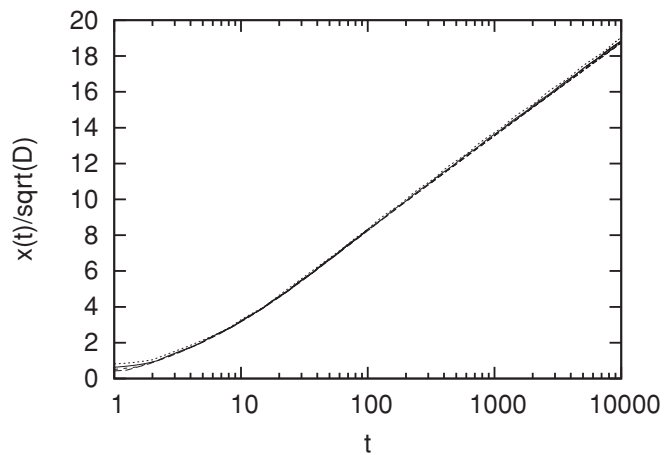

FIG. 3. Rescaled position of the interface $x(t)/\sqrt{D}$ as a function of time, for simulations in which $D = 0.5, 1, 2$, and 4. For longer times, the curves fall on top of each other, indicating that asymptotically $A \propto \sqrt{D}$.

(e.g. to create a O_2 molecule which is chemically neutral for C-particles) and with the C-particles is the reactive content of our model. Obviously the C particles must remain to define an interface at all, but we can imagine lowering very much the adsorption of the free O particles. In the extreme case we exclude the adsorption of free O particles by setting $\alpha = 0$. Then, we have $m(x,t) = 0$ always and everywhere which simplifies Eq. (1) somewhat. In the case of Dirichlet-type boundary condition $\rho(x = 0, t) = 1$, we basically have the transport of O particles through a layer of size $x(t)$ with the difference in concentration fixed (and equal to 1): we thus expect from Fick's law that the current $\dot{x}(t) \sim 1/x(t)$ is proportional to the concentration gradient which gives us $x(t) \sim \sqrt{t}$. We have checked that this behavior is indeed found for very small adsorption rates, $\alpha = 0$ and $\kappa = 0$. Figure 4 shows the numerical evidence.

On the other hand, with von Neumann boundary condition $\rho'(x = 0, t) = -J$ and for very small absorption rates $\alpha = 0$
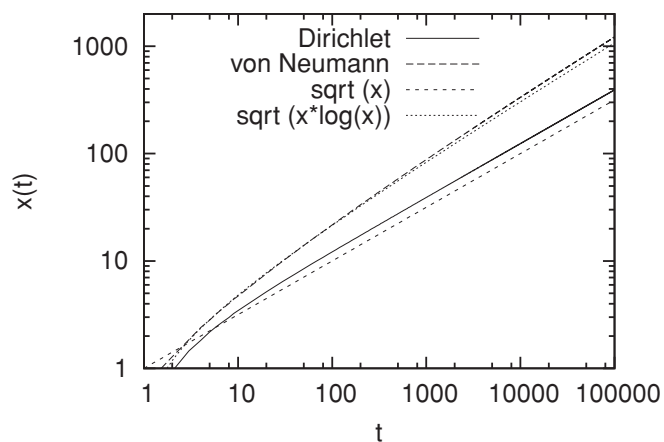

FIG. 4. Position of the interface $x(t)$ as a function of time, for simulations in which the adsorption of free oxygen is excluded. With Dirichlet boundary conditions, the asymptotic behavior can be well fitted by $x(t) \sim \sqrt{t}$; with von Neumann boundary conditions this becomes $x(t) \sim \sqrt{t \ln t}$.

and $\kappa = 0$, there is a continuous influx of free O particles leading to a concentration of them at the surface which increases in a power law fashion. That can be understood from the following calculation. Let us take $J = 1$ and consider the function

$$\rho_1(x,t) \equiv \sqrt{t}\, e^{-x/\sqrt{t}},$$

satisfying indeed $\partial_t \rho_1(x = 0,t) = -1$. Then, $\partial_t \rho_1(x,t) = \rho_1(x,t)/t\, [1 + x/\sqrt{4t}]$ and $\partial_x^2 \rho_1(x,t) = \rho_1(x,t)/t$, so that ρ_1 appears as a solution of the diffusion equation for $x \ll \sqrt{t}$. We thus conclude that $\rho_1(0,t)$ grows as $\sqrt{t}$. Numerically, we find that the lack of saturation of free O concentration at the exposed surface does not alter the asymptotic behavior of the interface, but it does lead to a logarithmic correction. The behavior is consistent with $x(t) \sim \sqrt{t} \ln t$. Also for von Neumann boundary conditions, numerical evidence is presented in Fig. 4.

IV. APPLICATION

Low dielectric constant (low-k) materials are typically used in semiconductor manufacturing to compensate for the RC delay and power consumption increase in microelectronic devices associated with their continuing scaling-down.[3,11] The microelectronics community has adopted k as a representation of the relative permittivity or dielectric constant in contrast to the scientific communities using ε_r. Nowadays, porous low-k dielectrics based on silica and silsesquioxanes with 10–15% of organic hydrophobic groups are the most favored class of materials for advanced interconnect technology nodes.[11] The hydrophobic groups are bonded to a Si atom in the $SiO_{4/2}$ matrix and can be represented as $O_3 \equiv SiCH_x$. To reach a k value below 3.0, introduction of artificial porosity is needed (the k value of air is close to 1).[3] Advanced low-k materials have a porosity of 25–50% and a typical pore size being close to 2–2.5 nm. Although the matrix of these materials has properties similar to traditional SiO_2, their chemical stability and reactivity strongly depend on porosity. Materials with interconnected pores are chemically active because of the high diffusion rate of active chemicals. In particular, the surface diffusion of adsorbed radicals is much faster than the desorption, which is our motivation not to include reversible adsorption-desorption in our model equations (1), see Refs. 12 and 13 for specific experimental estimates.

During device fabrication, the porous low-k dielectrics are exposed to various plasmas that might degrade their properties. The most challenging plasma treatment is related to plasmas based on oxygen- or hydrogen-containing chemistries that are used to remove organic photoresist masks used for pattern transfer from the low-k films.[14] The challenge arises from the similar chemical composition of the low-k film and the organic photoresist mask. Both materials contain C-H bonds. The plasma radicals that remove the organic mask also penetrate the porous low-k dielectric film destroying its $Si-CH_3$ bonds. This leads to the formation of polar Si-OH groups as a result of direct chemical reaction with active radicals or saturation of $\equiv Si\bullet$ broken bonds by OH groups from ambient moisture. The Si-OH groups are centers for further moisture adsorption.[15] The absorbed moisture with a k value of 80 can fill the whole open pore volume of the material

significantly increasing its k value which is summarized as damage.

Two commonly known approaches are used for the photoresist mask removal: (i) a low temperature, low pressure anisotropic plasma, where the photoresist is removed by an ion-assisted process, oxidizing or reducing plasma chemistries at low temperatures[10] and (ii) hydrogen-based downstream plasma (DSP) where the resist is removed at high temperatures by a thermally activated chemical process.[16] According to recent publications,[10,16] both approaches remove C from low-k materials. However, ion-assisted processes remove hydrophobic $Si-CH_3$ groups and graphitized C (residual C that remains after film fabrication), while a thermally activated chemical process with hydrogen plasma removes only graphitized C from low-k dielectrics. In both cases the depth of C-carbon removal can be directly measured with spectroscopic ellipsometry.[8,14] Various experimental results have shown the typical time dependence of the depth of C removal. In particular, the typical logarithmic time dependence was observed, as is the one we have derived in the present paper.

The depth of the plasma radical penetration in the low-k pores determines the extent of plasma damage. Clearly then, the role of Knudsen diffusion is important and our analysis in Sec. III A clarifies some aspects. For example, the extent of plasma damage can be a few times higher for mesoporous dielectrics with high porosity levels in comparison with nanoporous dielectric with low porosity levels.[17,18]

As a word of caution and limitations of our approach, plasma damage of low-k materials is a complex phenomenon that results in changes of their bonding structure and pore morphology.[3] The complexity also increases due to the fact that porous low-k dielectrics are usually amorphous materials with a random pore structure.[3] Our set of reaction-diffusion equations (1) can be generalized to include some of these aspects, but soon a more detailed simulation analysis becomes necessary.

V. CONCLUSION

The propagation of damage when a pristine material is exposed to diffusing and reacting particles saturates logarithmically. The initial position of the interface is diffusive $\sim \sqrt{t}$ but soon saturates $\sim \ln t$ when reactions prohibit the propagation of the damage. The problem can be modeled as a reaction-diffusion system of coupled differential equations where the position of the interface can be determined by viewing it as a Stefan problem. We have discussed Dirichlet and von Neumann boundary conditions, solved a linear approximation, and we have found the detailed influence of reactivities and diffusivity. Numerical integration of the coupled reaction-diffusion equations is in full accord with experimental findings in the context of microelectronic fabrication of low-k materials.

[1] J. Stefan, Annalen der Physik und Chemie **42**, 269 (1891).

[2] S. C. Gupta, *The Classical Stefan Problem: Basic Concepts, Modeling and Analysis* (Elsevier, New York, 2003).

[3] K. Maex *et al.*, J. Appl. Phys. **93**, 8793 (2003).

[4] Bartosz A. Grzybowski, *Chemistry in Motion: Reaction-Diffusion Systems for Micro- and Nanotechnology* (John Wiley and Sons, New York, 2009).

[5] V. I. Dybkov, *Reaction Diffusion and Solid State Chemical Kinetics*, 2nd ed. (IPMS Publications, Kiev, Ukraine, 2010).

[6] *Reaction-Diffusion Equations*, edited by K. J. Brown and A. A. Lacey (Oxford University Press, Oxford, 1990).

[7] A. Kolmogorov, I. Petrovsky, and N. Piskounov, Moscou Univ. Bull. Math. A **1**, 1 (1937).

[8] E. Kunnen, G. T. Barkema, C. Maes, D. Shamiryan, A. Urbanowicz, H. Struyf, and M. R. Baklanov, Microelectron. Eng. **88**, 631 (2011).

[9] Y. C. Kim and M. Boudart, Langmuir **7**, 2999 (1991).

[10] E. Kunnen *et al.*, J. Vac. Sci. Technol. B **28**, 450 (2010).

[11] W. Volksen, D. M. Miller, and G. Dubois, Chem. Rev. **110**, 56 (2010).

[12] P. Macko, P. Veis, and G. Cernogora, Plasma Sources Sci. Technol. **13**, 251 (2004).

[13] J. Marschall and J. E. Boulter, J. Phys. D: Appl. Phys. **39**, 3849 (2006).

[14] A. M. Urbanowicz *et al.*, Solid State Phenomena **134**, 317 (2008).

[15] M. R. Baklanov *et al.*, in Mat. Res. Soc., 2006.

[16] A. M. Urbanowicz *et al.*, Electrochem. Solid State Lett. **12**, H292 (2009).

[17] D. Shamiryan *et al.*, J. Vac. Sci. Technol. B **20**, 1923 (2002).

[18] D. Moore *et al.*, J. Vac. Sci. Technol. B **23**, 332 (2005).